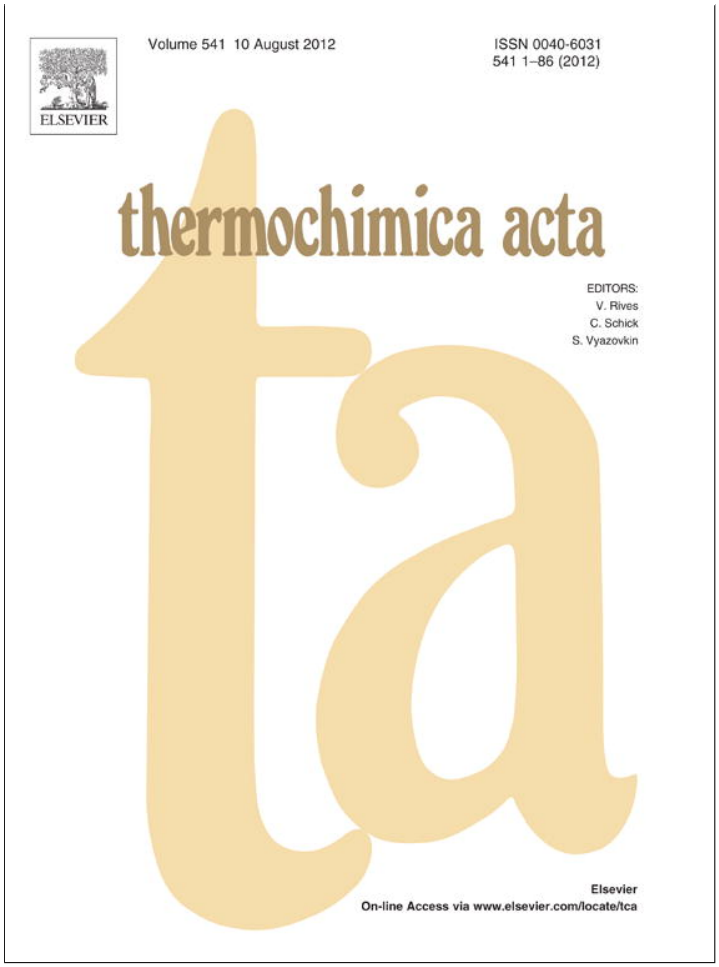

Thermochimica Acta 541 (2012) 8–14

Contents lists available at SciVerse ScienceDirect

Thermochimica Acta

journal homepage: www.elsevier.com/locate/tca

Melting of glass batch: Model for multiple overlapping gas-evolving reactions

Richard Pokorný [a], David A. Pierce [b], Pavel Hrma [b,c,*]

[a] Department of Chemical Engineering, Institute of Chemical Technology in Prague, Technická 5, 166 28, Prague 6, Czech Republic
[b] Pacific Northwest National Laboratory, Richland, WA 99352, USA
[c] Division of Advanced Nuclear Engineering, Pohang University of Science and Technology, Pohang, Republic of Korea

ARTICLE INFO

Article history:
Received 10 February 2012
Received in revised form 17 April 2012
Accepted 18 April 2012
Available online 26 April 2012

Keywords:
Overlapping reactions
Reaction kinetics
Kissinger method
Glass melting
Glass batch
TGA

ABSTRACT

In this study, we present a model for the kinetics of multiple overlapping reactions. Mathematical representation of the kinetics of gas-evolving reactions is crucial for the modeling of the feed-to-glass conversion in a waste-glass melter. The model simulates multiple gas-evolving reactions that occur during heating of a high-alumina high-level waste melter feed. To obtain satisfactory kinetic parameters, we employed Kissinger's method combined with least-squares analysis. The *n*th-order reaction kinetics with variable reaction order sufficed for obtaining excellent agreement with measured thermogravimetric analysis data.

1. Introduction

Successive and simultaneous reactions are common in reacting mixtures, and multiple overlapping reactions are typical in glass batches during their conversion to molten glass [1–19]. Yet hardly any mixture found in nature or in industrial technology has as many components and undergoes as many reactions as melter feeds during vitrification of nuclear wastes [20,21]. The waste itself contains compounds of 40–60 elements [22] that react with glass-forming additives on heating. Consequently, the non-isothermal thermogravimetric analysis (TGA) of high-level waste melter feeds reveals multiple overlapping peaks on the $d\alpha/dt$ versus T curve, where α is the conversion progress (degree of conversion), t is the time, and T is the temperature. These reactions occur within the cold cap, a layer of melter feed floating on the pool of molten glass in the melter [23,24]. The feed is charged on the top of the cold cap, where the temperature is ~100 °C, and as it moves towards the bottom, where the temperature is ~1000 °C, it is converted to glass [25,26]. A model for the conversion kinetics is needed for the cold cap model that in turn is a part of the model of the melter.

In this paper, we analyze the gas evolution process as recorded by the non-isothermal TGA. We do not attempt to assess the mechanisms of individual gas-evolving reactions from solid and liquid components, which are both successive and simultaneous and include the release of chemically bonded water, reactions of nitrates with organics, and reactions of molten salts with solid silica. We merely assume that the reactions are independent and their rates can be described by the equation $d\alpha_i/dt = f_i(\alpha_i)A_i \exp(-E_i/RT)$, where $f_i(\alpha_i) = (1-\alpha_i)^{n_i}$ is the nth-order reaction model, A is the pre-exponential factor, E is the activation energy, R is the universal gas constant, n is the (apparent) reaction order, and the subscript i stands for the ith reaction.

Our goal is to model the reaction kinetics in a way that is sufficient and adequate for modeling of the cold cap process. To this end, we deem the four-parameter simulation for each reaction satisfactory. These parameters are A_i, E_i, n_i, and w_i, the weight of the ith reaction (the fraction of the total mass loss caused by the ith reaction). Considering the number of reactions, this number of parameters is too large to effectively optimize with least-squares regression, especially for less distinct peaks. Therefore, we applied Kissinger's method [27] for the direct estimate of E_is based on the shift of the peak maximum temperature with the rate of heating and used least-squares optimization for the remaining parameters. The kinetics of reactions with overlapping peaks has been investigated since 1980s [28–36] and the two-step optimization was employed by several researchers [30–32,36].

2. Theory

The mechanisms of reactions that occur during the conversion of melter feeds to glass are complex. Fortunately, the *n*th-order

* Corresponding author at: Pacific Northwest National Laboratory, Richland, WA 99352, USA. Fax: +1 509 372 5997.
E-mail address: pavel.hrma@pnl.gov (P. Hrma).

0040-6031/$ – see front matter © 2012 Elsevier B.V. All rights reserved.
http://dx.doi.org/10.1016/j.tca.2012.04.019

Table 1
Melter feed composition in g/kg glass (main components).

Chemical	Mass	Chemical	Mass
$Al(OH)_3$	367.50	Na_2SO_4	3.57
H_3BO_3	269.83	$Bi(OH)_3$	12.80
CaO	60.80	Na_2CrO_4	11.13
$Fe(OH)_3$	73.83	KNO_3	3.03
Li_2CO_3	88.3	$NiCO_3$	6.33
$Mg(OH)_2$	1.70	$Pb(NO_3)_2$	6.17
NaOH	99.53	$Fe(H_2PO_2)_3$	12.43
SiO_2	305.03	NaF	14.73
$Zn(NO_3)_2{\cdot}4H_2O$	2.67	$NaNO_2$	3.40
$Zr(OH)_4{\cdot}0.654H_2O$	5.50	$Na_2C_2O_4{\cdot}3H_2O$	1.30
		Total	1349.6

reaction kinetics satisfactorily describes most of the gas-evolving melting reactions monitored by the TGA, allowing us to express the reaction rates as

$$\frac{d\alpha_i}{dt} = A_i(1-\alpha_i)^{n_i} \exp\left(-\frac{E_i}{RT}\right) \quad (1)$$

where α_i is the fraction of material reacted in the ith reaction.

In his seminal paper, Kissinger [27] developed a method to estimate E_i. Based on the determination of the temperature of the peak maximum for experiments carried out at different heating rates, he derived for E_i the formula

$$\frac{E_i}{R} = -\frac{d\left(\ln\left(\beta/T_{im}^2\right)\right)}{d(1/T_{im})} \quad (2)$$

where $\beta = dT/dt$ is the temperature increase rate and the subscript m denotes the peak maximum ($d^2\alpha_i/dt^2 = 0$). This approximate formula is highly applicable for batch melting reactions – see Section 5 for details.

If β is constant and $n \neq 1$, integration of Eq. (1) yields

$$\alpha_i = 1 - \left[1 + \frac{(n_i-1)A_i}{\beta}\int_0^T \exp\left(-\frac{E_i}{RT}\right) dT\right]^{1/(1-n_i)} \quad (3)$$

Following Kissinger, who used Murray and White's approximation for the exponential integral [37], Eq. (3) becomes

$$\alpha_i = 1 - \left[1 + \frac{(n_i-1)A_iRT^2}{E_i\beta}\left(1-\frac{2RT}{E_i}\right)\exp\left(-\frac{E_i}{RT}\right)\right]^{1/(1-n_i)} \quad (4)$$

This expression allows us to eliminate α from Eq. (1), thus expressing $d\alpha_i/dT$ as a function of T and β alone.

For multiple reactions that are mutually independent, we can write (using $T = T_0 + \beta t$)

$$\frac{d\alpha}{dT} = \frac{1}{\beta}\sum_i^N w_iA_i(1-\alpha_i)^{n_i} \exp\left(-\frac{E_i}{RT}\right) \quad (5)$$

where $\alpha = \Sigma\alpha_i$.

3. Experimental

Table 1 displays the composition of the melter feed used. As described elsewhere [21], this feed was formulated to vitrify a high-alumina high-level waste to produce glass of the composition (with mass fractions in parentheses): SiO_2 (0.305), Al_2O_3 (0.240), B_2O_3 (0.152), Na_2O (0.096), CaO (0.061), Fe_2O_3 (0.059), Li_2O (0.036), Bi_2O_3 (0.011), P_2O_5 (0.011), F (0.007), Cr_2O_3 (0.005), PbO (0.004), NiO (0.004), ZrO_2 (0.004), SO_3 (0.002), K_2O (0.001), MgO (0.001), and ZnO (0.001). This glass was designed for the Hanford Tank Waste Treatment and Immobilization Plant, currently under construction at the Hanford Site in Washington State, USA.

The simulated melter feed was prepared, as described by Schweiger et al. [21], as slurry that was dried at 105 °C overnight in an oven. For the TGA, feed samples of 10–60 mg were placed in a Pt crucible from TA Instruments© (New Castle, DE, U.S.A., SDT-Q600) and heated from ambient temperature (~25 °C) to 1200 °C at the rates 1, 5, 10, 15, 20, and 50 K/min.

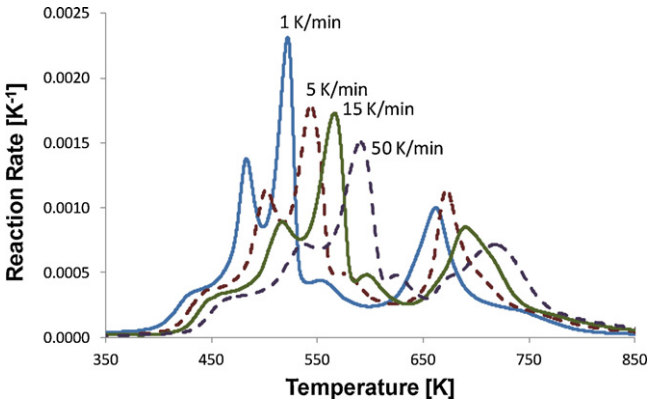

Fig. 1. Measured TGA curves for the melter feed heated at various rates.

Fig. 1 shows the TGA curves for the melter feed heated at several rates. As expected, the peaks shift to higher temperatures and the peak heights generally decrease as the rate of heating increases.

To deconvolute the TGA curve of $d\alpha/dT$ versus T for a series of βs, T_{im}s were determined as temperatures of the peak maxima or estimated for shoulders on larger peaks. From these data, with Eq. (2), we obtained E_is. Having predetermined E_is facilitated the application of the least squares analysis that we employed to fit the combined Eqs. (4) and (5) to measured $d\alpha/dT$ versus T data to obtain three independent parameters, A_i, n_i, and w_i, for each reaction.

4. Results

In our previous work [23], we fitted Eq. (5) with $n_i = 1$ to experimental data, taking advantage of the fact that with $n_i = 1$ one can calculate A_i using the formula $A_i = (\beta E_i/RT_{mi}^2)\exp(E_i/RT_{mi})$. Fig. 2 displays the results of the least-squares analysis for eight major reactions. Clearly, the agreement of measured and fitted curves is far from satisfactory: (1) the conversion rates are underestimated between peaks 1 and 2 and peaks 4 and 5; (2) the long tail of peak 8 is not well simulated; and (3) some fitted peaks overshoot the measured peaks.

To improve the model, we upgraded it to the nth-order reaction model and added reaction 1A between reactions 1 and 2. For the overlapped reactions, such as 1A, we obtained the T_m by subtracting the neighboring peaks as fitted from the measured curve. Fig. 3

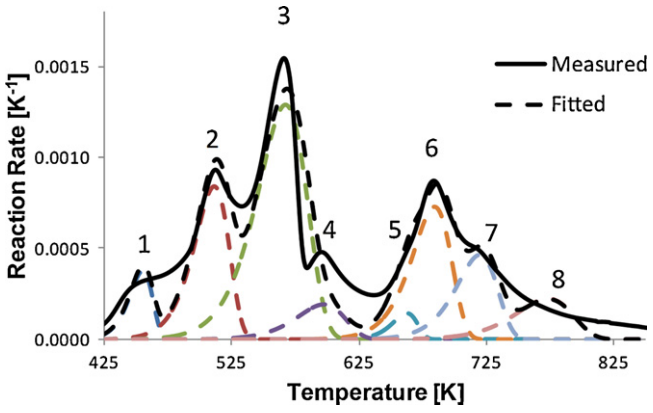

Fig. 2. Measured and fitted curves for the melter feed heated at 10 K/min for the first-order reaction model.

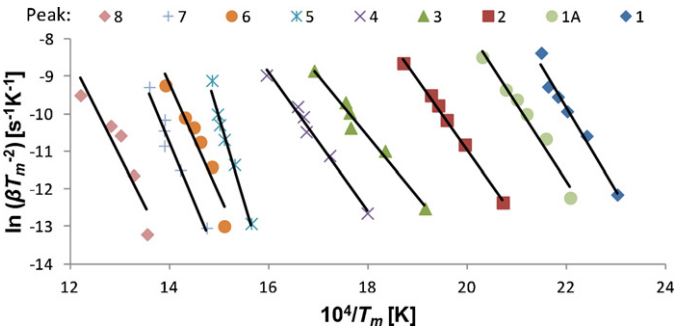

Fig. 3. Kissinger plot for the melter feed TGA peaks.

displays the Kissinger plot for all nine peaks. Table 2 lists the values of E calculated with Eq. (2), together with the standard deviations and the coefficients of determination, R^2. Table 3 lists the result of the least-squares analysis for $\beta = 15$ K/min.

Peak 8 possesses a long tail, which is probably caused by a process with a temperature-dependent E_8 or by a conglomerate of multiple reactions. The algorithm for the least-squares analysis simulates this long tail via a high value of the reaction order. The fitted n_is were also abnormally high for some other peaks (peak 5, as can be seen in Table 3, and peaks 1, 1A, and 7 in similar fits to some other heating rates). Because these elongated peaks unduly influence the neighboring peaks, we constrained n_is for peaks 1, 1A, 5, and 7 to $0 < n_i < 2$ but we left peak 8 to retain an unrestricted reaction order to represent the evolution of gas at high temperatures as faithfully as possible. Peak 8 gases might be responsible for foaming that affects, and perhaps even controls, the melting rate of the cold cap in the waste glass melter [23,25]. Tables 4–6 present the values of the kinetic coefficients A_i, n_i and the reaction weights, w_i, from fitting joined Eqs. (4) and (5) to the TGA curves.

Assuming that the kinetics of individual reactions does not change with the heating rate (Kissinger's formula is based on this assumption), the parameters A_i and n_i are independent of β. Indeed, as the very small values of standard deviation in Table 4 indicate, $\log(A_i)$ values are almost constant and their averages represent the averaged pre-exponential factors for individual reactions across the heating rates employed.

Somewhat larger standard deviations of n_is (up to 39%) indicate differences in the shapes of the peaks, but no trends can be discerned from the values. The n_i values of peaks with negligible weights (those in parentheses) were not included in the averages listed in Table 5. Note that $n_i = 2$ was imposed as the upper limit for peaks 1, 1A, 5 and 7.

On the other hand, w_i can vary with β, as consecutive reactions may be influenced by preceding ones, i.e., reactions that run at a lower temperature affect the reactions that follow them, especially when the heating rate is low. Accordingly, some reactions are not independent, but not to the extent that would invalidate the superposition relationship, Eq. (5).

Table 7 lists w_i values recalculated using the average values of A_i and n_i listed in Tables 4 and 5. Since w_i is the fraction of the material reacted by ith reaction, the sum of the w_is for all reactions, $w = 0.202 \pm 0.003$, represents the total mass loss during the heat treatment. Table 7 also lists the measured values of fractional mass loss, w_{TGA}. Fig. 4 plots the corresponding comparisons of measured and fitted TGA curves together with the peak deconvolution.

5. Discussion

As stated in Section 1, we have attempted to simulate the batch reaction kinetics for the modeling of the cold cap process regardless of the actual mechanisms of individual gas-evolving reactions. Our objective was to simulate the kinetics of reactions that evolve gases during batch heated at a rate that, though not constant, varies within the range covered by the TGA experiments. To this end, we chose the model-free Kissinger method combined with the least-squares curve fitting of the nth-order reaction kinetics. This approach is based on the following assumptions:

1. Batch reactions are kinetically simple.
2. Batch reactions can be treated as independent.
3. The nth-order reaction kinetics satisfactorily simulates measured data.

Table 2
Values of activation energy, E_i, its standard deviation, s, and coefficient of determination, R^2.

Peak	E_i [kJ/mol]	s [kJ/mol]	R^2
Peak 1	187	15	0.974
Peak 1A	170	14	0.973
Peak 2	156	5	0.996
Peak 3	134	10	0.977
Peak 4	152	9	0.986
Peak 5	373	27	0.979
Peak 6	248	35	0.926
Peak 7	263	26	0.962
Peak 8	216	50	0.862

Table 3
Optimized values of n_i, w_i, and $\log(A_i/s^{-1})$ for $\beta = 15$ K/min.

Peak	1	1A	2	3	4	5	6	7	8
n_i	2.73	1.83	1.09	0.51	2.11	12.03	0.79	1.66	3.44
w_i	0.010	0.008	0.026	0.051	0.036	0.016	0.010	0.031	0.016
$\log(A_i)$	20.18	17.05	14.06	10.49	11.57	27.79	17.13	17.73	12.86

Table 4
Values of $\log(A_i/s^{-1})$, average values, standard deviations, and relative standard deviations (RSD) for Peaks 1–8.

β [K/min]	1	1A	2	3	4	5	6	7	8
1	20.28	16.93	13.98	10.41	11.53	28.02	16.70	17.24	12.41
5	20.35	17.16	14.05	10.54	11.57	28.04	16.98	17.26	12.79
10	20.15	17.05	14.03	10.34	11.36	28.37	17.08	17.41	12.67
15	20.24	17.09	14.06	10.49	11.57	27.94	16.96	17.32	12.93
20	20.17	17.01	14.03	10.52	11.64	27.95	16.81	17.33	12.85
50	20.34	17.07	14.01	10.47	11.41	28.09	16.85	17.37	12.52
Average	20.26	17.05	14.03	10.46	11.51	28.07	16.90	17.32	12.69
Stdev	0.08	0.07	0.03	0.07	0.10	0.14	0.12	0.06	0.18
RSD	0.004	0.004	0.002	0.007	0.009	0.005	0.007	0.003	0.014

Table 5
Values of n_i, average values, standard deviations (values in parentheses were not included), and relative standard deviations for Peaks 1–8.

β [K/min]	1	1A	2	3	4	5	6	7	8
1	2.00	1.90	0.71	0.39	3.39	(1..19)	1.81	(0..10)	2.05
5	2.00	2.00	0.93	0.62	2.23	(0..61)	1.00	1.29	3.13
10	2.00	1.32	1.30	0.56	1.79	2.00	0.95	2.00	5.31
15	2.00	1.99	1.09	0.50	2.37	2.00	1.58	1.15	3.59
20	2.00	2.00	1.08	0.57	2.42	2.00	1.78	(0..55)	4.70
50	2.00	2.00	1.23	0.61	1.04	2.00	2.66	0.90	4.41
Average	2.00	1.87	1.06	0.54	2.21	2.00	1.63	1.33	3.87
Stdev	0.00	0.27	0.21	0.08	0.77	0.00	0.63	0.47	1.18
RSD	0.00	0.14	0.20	0.15	0.35	0.00	0.39	0.35	0.30

Table 6
Values of w_i and the total fraction reacted, $w = \Sigma w_i$, for Peaks 1–8.

β [K/min]	1	1A	2	3	4	5	6	7	8	w
1	0.009	0.008	0.026	0.052	0.041	0.000	0.045	0.000	0.018	0.198
5	0.007	0.011	0.027	0.055	0.037	0.000	0.034	0.015	0.022	0.207
10	0.008	0.007	0.031	0.049	0.031	0.002	0.023	0.028	0.023	0.203
15	0.008	0.010	0.025	0.051	0.038	0.001	0.036	0.009	0.023	0.202
20	0.008	0.010	0.023	0.049	0.040	0.003	0.042	0.002	0.025	0.203
50	0.007	0.012	0.024	0.055	0.026	0.010	0.050	0.005	0.013	0.201

Table 7
Values of w_i based on the average values of A_i and n_i listed in Tables 4 and 5, $w = \Sigma w_i$, and the total fractional mass loss as measured by TGA, w_{TGA}.

β [K/min]	1	1A	2	3	4	5	6	7	8	w	w_{TGA}
1	0.008	0.007	0.027	0.054	0.033	0.000	0.036	0.009	0.027	0.201	0.195
5	0.008	0.010	0.030	0.054	0.035	0.000	0.046	0.002	0.026	0.210	0.206
10	0.007	0.009	0.027	0.041	0.045	0.001	0.037	0.008	0.027	0.202	0.196
15	0.008	0.011	0.026	0.054	0.034	0.003	0.038	0.010	0.022	0.203	0.199
20	0.008	0.011	0.024	0.053	0.034	0.003	0.036	0.010	0.022	0.200	0.197
50	0.008	0.011	0.023	0.049	0.040	0.005	0.031	0.014	0.020	0.201	0.197

4. Errors caused by various approximations associated with Kissinger's formula are negligible.

These assumptions are discussed below.

5.1. Kinetic simplicity

The kinetic simplicity approximation is not only convenient, but is also useful for the cold cap model, which is complicated in various other aspects and requires an input that is as simple as possible. For kinetically simple reactions, the activation energy is constant. Thus, $\partial E_i/\partial \alpha_i = 0$ for $i = 1, 2, \ldots, N_R$, where N_R is the number of reactions. However, the diffusion-controlled kinetics of reactions in glasses, reactions in which one of the reactants is a molten salt with multiple cations, and the reactions producing multi-component solid-solution crystalline phases (spinel) are likely to be kinetically complex. Such phases are common during batch melting and the kinetic simplicity is an expedient approximation.

Kinetically complex reactions can be reasonably well approximated as kinetically simple if they occur within a narrow temperature interval. Reactions that run over a large interval of temperatures, such as reaction 8, are simulated as *n*th-order

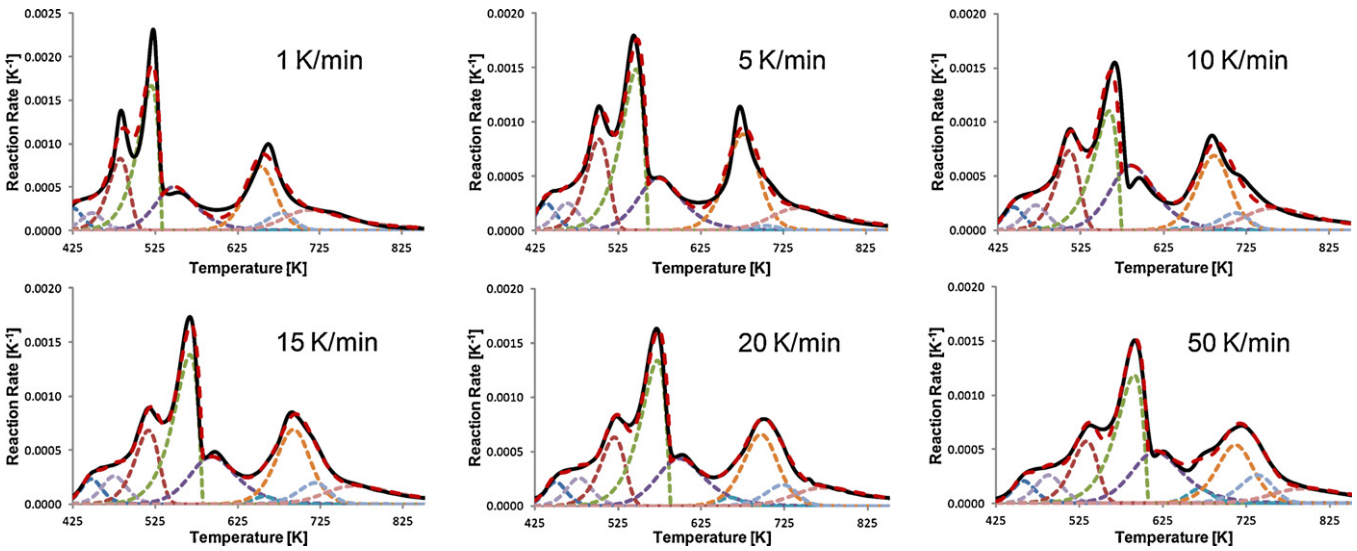

Fig. 4. Measured (solid line) and fitted (dashed line) TGA curves and deconvolution peaks for individual heating rates using average A_i and n_i.

reactions with an unrealistically large values of n. Gases evolved by this "tale" reaction contribute to foam generation, which is an important cold-cap phenomenon.

5.2. Independent reactions

Treating the discernible reactions as independent makes the analysis mathematically tractable. Reactions are independent if each reaction runs as if no other reactions were taking place in the mixture. This seems to be an oversimplification for glass batches, where individual reactions interact via shared reactants and reaction products affect the course of parallel and subsequent reactions. Interactions evolve differently in response to different temperature histories. Slow low-temperature reactions may run to a considerable extent during a slow heating, but may not occur to a measurable extent during a fast heating, thus changing the starting conditions for high-temperature reactions. The assumption of independence is acceptable within a relatively narrow range of β where very slow and very fast heating are avoided. The range of β expected within the cold cap is 10–45 K/min [25,26] and is narrower than the range used in our study (1–50 K/min).

A possible way of representing interactions would be adding interactive terms to Eq. (5), but this would severely complicate data evaluation while adding little value to the outcome considering various uncertainties and the simplicity requirement for the cold-cap modeling. An alternative way of recognizing, assessing, and possibly handling interactions is allowing the reaction weights in Eq. (5) to be functions of β while treating the values of A_i and n_i as independent of β. As data in Table 7 indicate, only w_1 appears strictly independent of β whereas w_5 clearly increases as β increases; w_i versus β for reactions 3, 4, and 6 fluctuate most likely because of experimental error. Two pairs of consecutive overlapping reactions seem to be coupled, namely, 1A with 2 and 7 with 8, a decrease in w_i of one member being compensated by an increase of the other or vice versa. However, these trends are weak and may result from random errors.

With a more precise data, one should be able to construct reasonable $w_i(\beta)$ approximation functions, at least for the heating rates of interest. Experimental errors that are responsible for w_i fluctuations can have various sources. Errors associated with the small sample size (the tiny Pt crucibles contained the sample mass of 30 mg in average, which is rather small for a mixture of granular materials) can be avoided by using an instrument that allows larger samples. As demonstrated in a previous study [20], temperature gradients affect data obtained with large samples of batches (20 g, compared with 20 mg of TGA samples). However, if the samples are not too large, one can argue that the vigorous gas evolution from the heated batches assists the heat transfer within the sample, thus suppressing the gradients. Another important issue is the diffusion of external gases into the sample that dilute the evolving gases, thus accelerating the reactions. This effect would influence small samples more than larger ones.

5.3. Kinetic model

We used the nth-order reaction kinetics to represent the batch reactions partly for its simplicity and partly out of necessity because, in spite of the vast literature, mechanisms of batch reactions are not known to the extent at which suitable mechanistic models can be constructed even for simple commercial batches with carefully controlled components. Soda-lime batches have been studied since the 19th century, yet authors of a recently published paper on reactions in a batch for a soda-lime glass [38] announced that they observed unexpected and "drastically different" phenomena that have a "profound influence" on reaction products. Whatever model we choose for such a reacting mixture, its parameters will be effective rather than physically meaningful. Though constructing molecular mechanisms of individual reactions would be desirable, our current objective is an application of the model for a specific response.

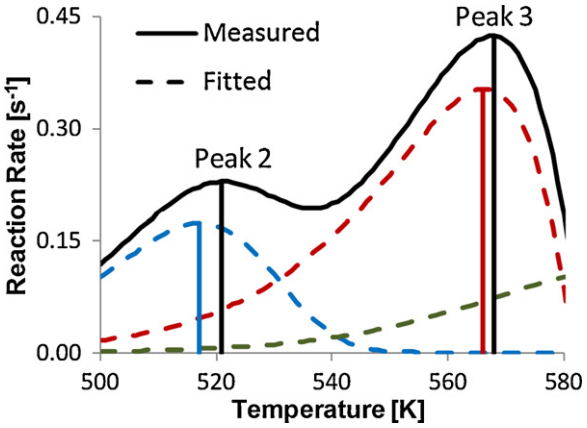

Fig. 5. Effect of peak overlapping on measured T_m.

5.4. Kissinger method limitations

Various sources of potential errors arise from approximations on which the Kissinger method is based:

1. approximation of the exponential integral as a truncated series;
2. approximations used in the development of Kissinger's formula, Eq. (2);
3. shift of T_m caused by peak overlapping.

For the "temperature integral," Kissinger used an approximation first derived by Murray and White [37] who performed integration by parts followed by the asymptotic expansion of the exponential integral. They truncated the series after the second term (not the first term, as Starink [39] states; nine years later, Coats and Redfern [40] published an identical formula that has been ever since associated with their names in the literature). According to Órfão [41], Murray and White's approximation for $E/RT > 20$ leads to 0.13% deviation of activation energy, which is well within the experimental accuracy.

Further, the Kissinger method omits the variations of α_m with β, E with α, and β with T (see Vyazovkin et al. [42]). Finally, when applying the Kissinger method to multiple reactions, we need to consider the shift of T_m caused by peak overlapping

As Budrugeac and Segal [43] have shown, the error caused by the variation of α_m with β is acceptable for most kinetic models if the reduced activation energy, $x_m = E/RT_m > 10$. For the nth order reaction kinetics, the relative error in E/R is $\varepsilon = -(R/E)\mathrm{d}\ln(-\mathrm{f}'_m)/\mathrm{d}(1/T_m) = (2/x)[2 - x/(1-n)]^{-1}$. According to this formula, $\varepsilon < 0.025$ for $x_m > 20$ and $n < 10$.

Regarding the limitations of the Kissinger method with respect to the variations of E with α and β with T, the former does not apply to kinetically simple reactions, and the latter is irrelevant to our study because, apart from minor fluctuations, the temperature increase rate was virtually linear in the instrument we used.

Fig. 5 illustrates the shift of T_m caused by peak overlapping. At some heating rates, this overlapping is evident in Fig. 4 in peaks 5, 6 and 7. To explore the effect of overlapping peaks on E_i, let us start from Eq. (5) in the form

$$\dot{\alpha} = w_i f_i(\alpha) A_i e^{-E_i/RT} + \sum_{j \neq i} w_j \dot{\alpha}_j \qquad (6)$$

Table 8
Values of E_i [kJ/mol] optimized for average reaction orders and pre-exponential factors.

Peak	1	1A	2	3	4	5	6	7	8
Kissinger	187	170	156	134	152	373	248	263	216
Fit to all data	187	170	156	134	152	376	248	263	215
Average of separate fits	187	170	156	134	152	374	248	263	216

where $\dot{\alpha}_j = w_j f_j(\alpha) A_j e^{-E_j/RT}$ and the dot above the symbol denotes the time derivative. Applying to Eq. (6) the condition for the ith reaction maximum on the TGA curve, i.e., $\alpha = 0$ at each $T = T_{mi}$, we obtain

$$0 = \dot{\alpha}_i(T_{mi}) \left[\frac{E_i \beta}{RT_{mi}^2} + w_i f_i'(\alpha_{mi}) A_i e^{-E_i/RT_{mi}} \right] + \sum_{j \neq i} w_j \ddot{\alpha}_j(T_{mi}) \tag{7}$$

where the prime denotes the derivative. Rearranging and taking a logarithm, Eq. (7) becomes

$$\ln \frac{\beta}{T_{mi}^2} + \ln \left[1 + \frac{RT_{mi}^2 \sum_{j \neq i} w_j \alpha_j''(T_{mi})}{E_i \alpha_i'(T_{mi})} \right] = \ln \left[-\frac{w_i f_i'(\alpha_{mi}) A_i R}{E_i} \right] - \frac{E_i}{RT_{mi}}. \tag{8}$$

where $\alpha'' = d^2\alpha/dT^2$. The Kissinger formula now assumes the form

$$-\frac{E_i}{R} = \frac{\mathrm{d} \ln \left(\beta / T_{mi}^2 \right)}{\mathrm{d}(1/T_{mi})} + \frac{\mathrm{d} \ln \left[1 + \left(RT_{mi}^2 \sum_{j \neq i} w_j \alpha_j''(T_{mi}) / E_i \alpha_i'(T_{mi}) \right) \right]}{\mathrm{d}(1/T_{mi})} - \frac{\mathrm{d} \ln \left[-f_i'(\alpha_{mi}) \right]}{\mathrm{d}(1/T_{mi})}. \tag{9}$$

We have already shown that the third term on the right hand side can be neglected for high-temperature reactions. The second term is negligible if

$$\sum_{j \neq i} w_j \alpha_j''(T_{mi}) << \frac{E_i}{RT_{mi}^2} \alpha_i'(T_{mi}). \tag{10}$$

Then Eq. (8) becomes Eq. (2). If only two peaks overlap, inequality (10) reduces to $w_j \alpha_j''(T_{mi}) << \left(E_i / RT_{mi}^2 \right) \alpha_i'(T_{mi})$.

Let us check this inequality with peaks 2 and 3 as shown in Fig. 5, where the first maximum associated with reaction 2 ($i \equiv 2$) is shifted to a higher temperature because of the overlapping peak of reaction 3 ($j \equiv 3$). With the values $w_3 = 0.054$ and $\alpha_3''(T_{m2}) = 1.67 \times 10^{-4}$, we get $w_2 \alpha_2''(T_{m2}) = 9.03 \times 10^{-6}\,\mathrm{K}^{-2}$; with $E_2 = 156$ kJ/mol, $T_{m2} = 521$ K, and $\alpha_2'(T_{m2}) = 0.665$, we have and $E_2 R^{-1} T_{m2}^{-2} \alpha_2'(T_{m2}) = 4.60 \times 10^{-2}\,\mathrm{K}^{-2}$. Hence, inequality (10) is satisfied for this example. It is also likely to be satisfied if the central peak overlaps with two peaks on the opposite sides. Then the two values of $w_j \alpha_j''(T_{mi})$ of the side peaks have opposite signs.

If the neighboring peaks are close to each other and the slope $\alpha_j'' = \mathrm{d}\alpha_j'/\mathrm{d}T$ at $T = T_{mi}$ is large, inequality (10) is not satisfied. As Wilburn [33] showed, it is impossible to determine the kinetic coefficients of such reactions. But the hidden peaks (shoulders) can emerge as the heating rate changes if the reactions have different activation energies. If a peak becomes concealed within the experimental range of β, the kinetic model can still be used for mathematical representation of the reacting mixture if the actual rate of heating remains confined within the experimental one.

To verify that Kissinger's formula provides correct values of E in spite of the T_m shift, we optimized E_is directly from data. Separate fitting to each heating rate with the average values of A_i and n_i and the w_i values listed in Table 7 resulted in fluctuating E_is with averages close to the values from Kissinger's formula, though with lower standard deviations. Fitting the model to all data for all heating rates at once with the same A_i, n_i and the w_i values as for the separate fitting resulted in E_is that were close to both the averages and E_is obtained using Kissinger's method – see Table 8. Thus, additional fitting did not bring any improvement worth considering.

Because of the compensation effect between E_i and A_i that results from the relatively narrow temperature interval in which the ith reaction starts and is complete, nearly the same fit can be obtained from relatively wide ranges of E_i and A_i combinations [28]. For this reason, Kissinger's method appears preferable to fitting of E_i and A_i simultaneously. A similar conclusion seems to have been reached by others [30–33,36].

5.5. Kinetic prediction

The model we have developed for the batch melting reactions is not intended for extrapolation with respect to experimental variables. In particular, it is limited to the experimentally applied heating rates, and, consequently, to the experimental temperature interval. For example, it is not expected to be applicable to an extremely fast heating followed by a constant temperature heat treatment at a very high temperature.

Kinetic prediction applies to our model in a limited sense: the model is intended for interpolation rather than extrapolation. While extreme heating rates are unlikely to occur within the cold cap, the melter feed experiences changing heating rates as it proceeds from batch to molten glass. Since the heating rate vary within relatively narrow limits during the conversion, the kinetic relationship, i.e., Eq. (5) with the values of parameters listed in Tables 4, 5 and 7, is expected to provide the reaction term for the mass balance equation used in the mathematical model of the cold cap [25,26].

6. Conclusions

The kinetic model with empirical reaction order yields a reasonable simulation for the kinetics of multiple overlapping reactions that are typical of melting glass batches. The nth-order reaction model employed was successful even though it does not represent the mechanism of reactions between multiple granular solids and ionic and glass-forming melts produced in glass batches at higher temperatures. Thus, each reaction was sufficiently characterized with four coefficients, i.e., the activation energy, the pre-exponential factor, the reaction order, and the weight (the fraction reacted), of which only the weight is a weak function of the rate of heating. To avoid problems with the compensation effect between the activation energy and the pre-exponential factor, we successfully combined Kissinger's method with least-squares optimization. The three kinetic coefficients plus the reaction weights thus obtained can be used in an advanced model for glass melting in the cold cap.

Acknowledgments

This research was supported by the U.S. Department of Energy Federal Project Office Engineering Division for the Hanford Tank

Waste Treatment and Immobilization Plant and by the WCU (World Class University) program through the National Research Foundation of Korea funded by the Ministry of Education, Science and Technology (R31 – 30005). Richard Pokorný is pleased to acknowledge support from Czech Grant Agency (GACR No. P106/11/1069). The authors are grateful to Albert Kruger for his assistance and guidance and to Dong-Sang Kim and Jaehun Chun for insightful discussions.

References

[1] F.W. Wilburn, C.V. Thomasson, The application of differential thermal analysis and thermogravimetric analysis to the study of reactions between glass-making materials. Part 1. The sodium carbonate-silica system, J. Soc. Glass Technol. 42 (1958) 158T–175T.
[2] C.V. Thomasson, F.W. Wilburn, The application of differential thermal analysis and thermogravimetric analysis to the study of reactions between glass-making materials. Part 2. The calcium carbonate–silica system with minor batch additions, Phys. Chem. Glasses 1 (1960) 52–69.
[3] F.W. Wilburn, C.V. Thomason, The application of differential thermal analysis and thermogravimetric analysis to the study of reactions between glass-making materials. Part 3. The sodium carbonate-silica system, Phys. Chem. Glasses 2 (1961) 126–131.
[4] F.W. Wilburn, C.V. Thomason, The application of differential thermal analysis and differential thermogravimetric analysis to the study of reactions between glass-making materials. Part 4. The sodium carbonate–silica–alumina system, Phys. Chem. Glasses 4 (1963) 91–98.
[5] F.W. Wilburn, S.A. Metcalf, R.S. Warburton, Differential thermal analysis, differential thermogravimetric analysis, and high temperature microscopy of reactions between major components of sheet glass batch, Glass Technol. 6 (1965) 107–114.
[6] W.R. Ott, M.G. McLaren, W.B. Harsell, Thermal analysis of lead glass batch, Glass Technol. 13 (1972) 154–160.
[7] E. Bader, Combined method of differential thermal analysis and evolved gas analysis with the heat conductivity detector for study of Pyrex batches, Silikattechnik 28 (1977) 23–28.
[8] E. Bader, Thermoanalytical investigation of melting and fining of Thüringen laboratory glassware, Silikattechnik 29 (1978) 84–87.
[9] E. Bader, Melting reactions in B-3.3-glass batches with soda and sodium nitrate as alkali sources, Silikattechnik 30 (1979) 112–115.
[10] E. Bader, Effect of cullet on melting reactions in B-3.3- and Na–Ca–silica glass batches, Silikattechnik 30 (1979) 269–272.
[11] J. Mukerji, A.K. Nandi, K.D. Sharma, Reaction in container glass batch, Ceram. Bull. 22 (1979) 790–793.
[12] O. Abe, T. Utsunomiya, Y. Hoshino, The reaction of sodium nitrate with silica, Bull. Chem. Soc. Jpn. 56 (1983) 428–433.
[13] T.D. Taylor, K.C. Rowan, Melting reactions of soda-lime-silicate glasses containing sodium sulfate, J. Am. Ceram. Soc. 66 (1983), C-227–228.
[14] M. Lindig, E. Gehrmann, G.H. Frischat, Melting behavior in the system SiO_2–K_2CO_3–$CaMg(CO_3)_2$ and SiO_2–K_2CO_3–PbO, Glastech. Ber. 58 (1985) 27–32.
[15] C.A. Sheckler, D.R. Dinger, Effect of particle size distribution on the melting of soda-lime-silica glass, J. Am. Ceram. Soc. 73 (1990) 24–30.
[16] K.S. Hong, R.E. Speyer, Thermal analysis of reactions in soda-lime-silicate glass batches containing melting accelerants. I. One- and two-component systems, J. Am. Ceram. Soc. 76 (1993) 598–604.
[17] K.S. Hong, S.W. Lee, R.E. Speyer, Thermal analysis of reactions in soda-lime-silicate glass batches containing melting accelerants. II. Multicomponent systems, J. Am. Ceram. Soc. 76 (1993) 605–608.
[18] M.E. Savard, R.E. Speyer, Effect of particle size on the fusion of soda–lime–silicate glass containing NaCl, J. Am. Ceram. Soc. 76 (1993) 671–677.
[19] H.S. Ray, Introduction to Melts: Molten Salts, Slags and Glasses, Allied Publishers Pvt Ltd., 2006.
[20] P. Hrma, M.J. Schweiger, C.J. Humrickhouse, J.A. Moody, R.M. Tate, T.T. Rainsdon, N.E. TeGrotenhuis, B.M. Arrigoni, J. Marcial, C.P. Rodriguez, B.H. Tincher, Effect of glass-batch makeup on the melting process, Ceram. Silik. 54 (2010) 193–211.
[21] M.J. Schweiger, P. Hrma, C.J. Humrickhouse, J. Marcial, B.J. Riley, N.E. TeGrotenhuis, Cluster formation of silica particles in glass batches during melting, J. Non-Cryst. Solids 356 (2010) 1359–1367.
[22] D. Kim, M.J. Schweiger, C.P. Rodriguez, W.C. Lepry, J.B. Lang, J.V. Crum, J.D. Vienna, F.C. Johnson, J.C. Marra, D.K. Peeler, Formulation and characterization of waste glasses with varying processing temperature, PNNL-20774, EMSP-RPT-00, 2011.
[23] P. Hrma, D.A. Pierce, R. Pokorný, Thermal analysis of waste glass melter feeds, in: Proceedings of the International Symposium on Radiation Safety Management, Gyeongju, Republic of Korea, November 2–4, 2011, pp. 217–222.
[24] D.A. Pierce, P. Hrma, J. Marcial, B.J. Riley, M.J. Schweiger, Effect of alumina source on ease of melting of glass batch, Int. J. Appl. Glass Sci. 3 (2012) 59–68.
[25] R. Pokorný, P. Hrma, Mathematical modeling of cold cap, submitted.
[26] P. Hrma, A.A. Kruger, R. Pokorný, Nuclear waste vitrification efficiency: cold cap reactions, J. Non-Cryst. Solids (2012), http://dx.doi.org/10.1016/j.jnoncrysol.2012.01.051.
[27] H.E. Kissinger, Reaction kinetics in differential thermal analysis, Anal. Chem. 29 (1957) 1702–1706.
[28] V. Marcu, E. Segal, Kinetic analysis of sequence of two consecutive reactions from thermogravimetric data under non-isothermal conditions. I. Calculated thermograms, Thermochim. Acta 35 (1980) 43–49.
[29] N. Ito, Separation of DTA peaks of a multistage reaction, Thermochim. Acta 76 (1984) 121–126.
[30] S. Boy, K. Böhme, Kinetic analysis of additively overlapping reactions. Part 1. Description of an optimization method and its use for the separation of peaks, Thermochim. Acta 75 (1984) 263–273.
[31] J.M. Criado, M. González, A. Ortega, C. Real, Discrimination of the kinetic model of overlapping solid-state reactions from non-isothermal data, J. Therm. Anal. Calorim. 34 (1988) 1387–1396.
[32] V. Slovák, Determination of kinetic parameters by direct non-linear regression from TG curves, Thermochim. Acta 372 (2001) 175–182.
[33] F.W. Wilburn, Kinetics of overlapping reactions, Thermochim. Acta 354 (2000) 99–105.
[34] F. Barbadillo, A. Fuentes, S. Naya, R. Cao, J.L. Mier, R. Artiaga, Evaluating the logistic mixture model on real and simulated TG curves, J. Therm. Anal. Calorim. 87 (2007) 223–227.
[35] R. Robinson, F. Patisson, B. Björkman, Low temperature reactivity in agglomerates containing iron oxide, J. Therm. Anal. Calorim. 103 (2011) 185–193.
[36] S. Primig, H. Leitner, Separation of overlapping retained austenite decomposition and cementite precipitation reactions during tempering of martensitic steel by means of thermal analysis, Thermochim. Acta 526 (2011) 111–117.
[37] P. Murray, J. White, Kinetics of the thermal dehydration of clays. IV. Interpretation of the differential thermal analysis of the clay minerals, Trans. Br. Ceram. Soc. 54 (1955) 204–237.
[38] E. Gouillart, M.J. Toplis, J. Grynberg, M.-H. Chopinet, E. Sondergard, L. Salvo, M. Suéry, M. Di Michiel, G. Varoquaux, In situ synchrotron microtomography reveals multiple reaction pathways during soda–lime glass synthesis, J. Am. Ceram. Soc. 95 (2012) 1–4.
[39] M.J. Starink, The determination of activation energy from linear heating rate experiments: a comparison of the accuracy of isoconversion methods, Thermochim. Acta 404 (2003) 163–176.
[40] A.W. Coats, J.P. Redfern, Kinetic parameters from thermogravimetric data, Nature 201 (1964) 68–69.
[41] J.J.M. Órfão, Review and evaluation of the approximations to the temperature integral, AIChE J. 53 (2007) 2905–2915.
[42] S. Vyazovkin, A.K. Burnham, J.M. Criado, L.A. Pérez-Maqueda, C. Popescu, N. Sbirrazzuoli, ICTAC Kinetics Committee recommendations for performing kinetic computations on thermal analysis data, Thermochim. Acta 520 (2011) 1–19.
[43] P. Budrugeac, E. Segal, Applicability of the Kissinger equation in thermal analysis, J. Therm. Anal. Calorim. 88 (2007) 703–707.